Modulation instability in nonlinear metamaterials modeled by a cubic-quintic complex Ginzburg-Landau equation beyond the slowly varying envelope approximation

Laure Tiam Megne,[1,2,*] Conrad Bertrand Tabi [3,†] and Timoléon Crépin Kofane[1,2,3,‡]

[1]*Laboratory of Mechanics, Department of Physics, Faculty of Science, University of Yaoundé I, P.O. Box 812, Yaoundé, Cameroon*
[2]*Centre d'Excellence Africain en Technologies de l'Information et de la Communication, University of Yaoundé I,*
P.O. Box 812, Yaoundé, Cameroon
[3]*Department of Physics and Astronomy, Botswana International University of Science and Technology,*
Private Mail Bag 16 Palapye, Botswana

Considering the theory of electromagnetic waves from the Maxwell's equations, we introduce a (3+1)-dimensionsal cubic-quintic complex Ginzburg-Landau equation describing the dynamics of dissipative light bullets in nonlinear metamaterials. The model equation, which is derived beyond the slowly varying envelope approximation, includes the effects of diffraction, dispersion, loss, gain, cubic, and quintic nonlinearities, as well as cubic and quintic self-steepening effects. The modulational instability of the plane waves is studied both theoretically, using the linear stability analysis, and numerically, using direct simulations of the Fourier space of the proposed nonlinear wave equation, based on the Drude model. The linear theory predicts instability for any amplitude of the primary wave. Also, in the linear stability analysis, self-steepening effects of different orders are confronted and one discusses their effects on the behavior of the gain spectrum under both normal and anomalous group-velocity dispersion regimes. Analytical results are equally confronted to direct numerical simulations and fully agree with the predictions from the gain spectra. Modulational instability is manifested by clusters of solitons and multihump and dromion-like structures, whose emergence and features depend not only on system parameters, such as the cubic and quintic self-steepening coefficients, but also on the propagation distance under a suitable balance between nonlinear and dispersive effects.

I. INTRODUCTION

The dynamics of pulses propagating in nonlinear metamaterials (MMs) has been a major area of research given its potential application in optical communication systems [1–6]. Metamaterials, which are an arrangement of artificial structural elements, designed to achieve advantageous and/or unusual (electromagnetic) properties, are often associated with negative refraction, and sometimes they can be called negative index materials (NIM) or left-handed materials, with simultaneous negative effective permittivity and negative effective permeability [7–12]. The application possibilities of metamaterials are found in industrial sectors like information and communication technologies, space, security, and defense, but also applications in health, energy, and environmental areas are foreseen. Examples of devices that have been realized during the past few years are sensors, superlensing, cloaking, and light emitting diodes or cavities for low-threshold lasers and these were based on controlling the wave propagation and used dynamic, reconfigurable, and tunable materials.

It is known that the self-modulation of waves propagating in nonlinear magnetic metamaterials is governed by the nonlinear Schrödinger (NLS) equation [13]. This self-modulation of the carrier wave leads to a spontaneous energy localization via the generation of localized envelope structures (envelope solitons). The NLS equation has exact soliton solutions that correspond to a balance between nonlinearity and dispersion in the case of temporal solitons or between nonlinearity and diffraction in the case of spatial solitons. Inverse scattering theory has been applied with great success to the NLS equation, and solutions are dark and bright solitons, with *tanh* and *sech* profiles, respectively. Some interesting results, including the stability conditions of electromagnetic wave and physical conditions leading to rogue wave trains generation, such as Akhmediev-Peregrine waves and Akhmediev wave trains and Kuznetsov-Ma waves, when the quintic nonlinearity comes into play for negative index regime and amplified for absorption regime at a specific frequency range, have been obtained [14–16]. At the same time, Lazarides and Tsironis [17] have shown that for specific parameter choices, corresponding to either an isotropic, homogeneous left-handed or a right-handed medium, Maxwell's equations with nonlinear constitutive relations lead naturally to a system of coupled NLS equations for the envelopes of the propagating electric and magnetic fields, with dark and bright soliton solutions, respectively. Another class of equations of particular interest is the cubic complex Ginzburg-Landau (CGL) equation

---

*Corresponding author: tiamlaure@yahoo.fr
†conrad@aims.ac.za, tabic@biust.ac.bw
‡tckofane@yahoo.com

and its variants [18]. Such equations adequately model the dissipative solitons generation and propagation in systems including nanophotonics, nanoplasmonics, plasmas, and fluids, as well as superconductivity, superfluidity, elementary particles, electrical transmission line, doped optical fiber, and biological systems, respectively [18]. In particular, a (3+1)D cubic-quintic CGL equation modeling dissipative spatiotemporal solitons in negative-refractive-index materials, as well as positive-refractive-index materials, has been derived [19].

To enlarge the information capacity, it is necessary to transmit ultrashort optical solitons at high bit rate in the picosecond and femtosecond regimes, and several new effects greatly influence their propagation properties. For example, in the picosecond regimes, the pulse propagation in nonlinear optical communication systems are usually of Kerr type, and the dynamics of light pulses, whose description is based on the slowly varying envelope approximation (SVEA) or quasimonochromatic approximation leads to the NLS or CGL equation with cubic nonlinear terms. The validity of the NLS and CGL equations as reliable models is dependent on the assumption that the spatial width of the soliton is much larger than the carrier wavelength, which is equivalent to the condition that the width of the soliton frequency spectrum is much less than the carrier frequency. In other words, the NLS and CGL equations describe the evolution of an envelope function which is assumed to vary slowly over an optical cycle. In the femtosecond regimes, the materials used in optical systems are of non-Kerr type. This has been made more visible, thanks to recent developments in ultrashort pulse generation techniques that resulted in the production of sub-10-fs optical pulses [20–25]. It has been shown that the SVEA breaks down for these ultrashort optical pulses or even for initial pulses that are many optical cycles long [26–30]. Indeed, Rothenberg [26] has shown that the three-dimensional NLS equation derived in the SVEA is not adequate for describing the self-focusing of femtosecond pulses in dispersive media and that the breakdown of this approximation occurs for pulses much longer than an optical cycle. Furthermore, Oughstun and Xiao [27] have considered an input pulse envelope propagating in the positive z direction through a linear dielectric whose frequency dispersion is described by the double resonance Lorentz model with complex index of refraction. The dynamical field evolution shows that at three, five, and seven absorption depths into the dispersive medium, the SVEA remains accurate in its description of the main body of the pulse that is oscillating at (or very near to) the input carrier frequency. However, at 10 absorption depths into the dispersive medium, the accuracy of the SVEA is seen to have completely broken down.

A theoretical model based on a general three-dimensional wave equation, that includes the effects of space-time focusing and self-steepening in a self-consistent fashion, was derived by Brabec and Krausz [31], which received the name "slowly evolving wave approximation" (SEWA) by the previous authors, that extends the NLS equation for an accurate description of the evolution of the wave packet envelope down to pulse durations as short as one carrier oscillation cycle. Porras [32] has found ultrashort pulsed Gaussian beam solutions of the three-dimensional envelope equation in dispersive media beyond the SVEA that represents few-cycle

pulsed light beams propagating under the joint effects material gain (losses), phase and gain dispersion, diffraction, with the proper inclusion of space-time focusing. Based on what they called the generalized few-cycle envelope approximation, Kinsler and New [33] presented a comprehensive framework for treating the nonlinear interaction of few-cycle pulses using an envelope description that goes beyond the traditional SVEA. Then, they applied it to both optical nondegenerate parametric amplification and the optical parametric oscillator, where no approximations are made until the final stage when a particular problem is considered. At the same time, Ranka and Gaeta [34] showed theoretically that for ultrashort pulses that were initially much longer than a single optical cycle, the pulse-splitting dynamics could exhibit a significant deviation from the results predicted by the NLS equation. These predictions were found to be in excellent agreement with experiments that they performed in bulk fused silica. In the same context, by using the SEWA, it has been shown, based on an extended NLS equation, coupled with the density of electrons produced mainly by multiphoton band-to-band transitions, that intense ultrashort infrared laser pulses propagating through the fused silica over several Rayleigh lengths self-organize in narrow filaments with high peak intensity, and which persist over exceptionally long distances due to a quasidynamic equilibrium between multiphoton ionization and self-focusing [35]. Akozbek *et al.* [36] presented numerical results on the propagation of femtosecond pulses in air including multiphoton ionization, group velocity dispersion, space-time focusing, self-steepening, Raman response, and higher-order quintic defocusing term. They showed that a close connection exists between the self-steepening of the pulse and white-light generation in air and white-light generation in solids. Gaeta [37] also reported a theoretical investigation of the nonlinear propagation of femtosecond pulses tuned near the zero-dispersion point of a fiber waveguide in which a white-light continuum was generated in a microstructured fiber. In addition, using the Maxwell equations, a basic equation modeling the propagation of ultrashort optical solitons in optical fiber, named the higher-order $(3 + 1)$ D cubic-quintic-septic CGL equation was derived by Djoko and Kofané [38], explaining the spatiotemporal dynamics of bell-shaped dissipative light bullets; double, triple, and quadruple bullet complexes [38]; stable stationary and pulsating solutions, 3D stable vortex [39]; double, quadruple, 6-fold, 8-fold, and 10-fold bullet complexes [40], including also self-trapped, necklace-ring, ring-vortex solitons, uniform-ring beams, and spherical and rhombic distributions of light bullets; and fundamental and cluster solitons [41].

Various potential applications of MM have been proposed and studied [42–47]. First, for propagation of ultrashort pulses in MMs with a nonlinear electric polarization, it has been demonstrated that the linear dispersive magnetic permeability is incorporated into the nonlinear polarization, resulting in a controllable self-steepening (SS) effect and a series higher-order dispersive nonlinear term in the propagation models [42,43]. So, various generalized NLS equations, suitable for few-cycle pulse propagation in the MMs without [44,45], and with delayed Raman response, were reported [46]. Solitary wave solution of the generalized NLS equation for dispersive permittivity and permeability using a scaling transformation

and coupled amplitude-phase formulation was presented by Sarma [47]. Second, one of the key issues of solitary wave theory is the universal modulation instability (MI) phenomena which is one of the most fundamental processes in nonlinear wave systems in nature. MI, which is an indispensable mechanism for understanding pattern formation in a uniform medium, is a process in which the amplitude and phase modulations of a wave grow under the combined effects of nonlinearity and diffraction or dispersion in a spatially nonlinear field. It refers to the exponential growth of weak perturbations through the amplification of sideband frequencies. Hence, the MI provides a natural means of generating ultrashort pulses at ultrahigh repetition rates and is thus potentially useful for the development of high-speed optical communication systems. In optics, MI has constituted a wide field of intense theoretical and experimental research including ultrafast pulse generation [48], supercontinuum generation [49,50], four-wave mixing [50,51], Bragg gratings [52], parametric oscillators [53,54], optical fiber [55–59], and so on. The phenomenon of MI has received a lot of attention in the context of MM, specifically in the NIM [60–63]. Since then, MI has been extended intensively for few-cycle optical pulses with pulse duration as short as one carrier oscillation cycle [64–75].

The main objective of the present work is that, motivated by both features, that is, few-cycle regimes and MI, we fo-

cus on the issue of how MI, which is closely related to the existence of optical solitons, may play a key role in the generation of few-cycle pulses and their propagation through MMs. In our contribution, we start with the Maxwell's equations describing the response of the nonlinear medium to an electromagnetic wave. Then we report on the derivation of the (3+1)D cubic-quintic CGL equation, beyond the SVEA, which is further used to discuss theoretically and numerically MI of few-cycle pulses on this equation. We examine plane wave stability by means of both a rigorous analysis of linearized equations for small perturbations and using direct numerical simulations to support our analytical predictions.

The rest of the paper is organized as follows. In Sec. II, we derive a (3+1)D cubic-quintic CGL equation describing the dynamics of dissipative light bullets in nonlinear metamaterials beyond the SVEA, under the joint effects of diffraction, dispersion, loss, gain, cubic and quintic nonlinearities, and cubic and quintic self-steepening terms. In Sec. III, the linear stability analysis of the MI is addressed, and instability zones as well as the analytic expressions of the gain of MI are obtained. Numerical simulations, based on analytical findings, are carried out on the (3+1)D cubic-quintic CGL equation using the split-step Fourier method. Particular attention is paid to the joint effects of the cubic and quintic self-steepening parameters. Some concluding remarks are given in Sec. IV.

II. THEORETICAL MODEL: THE (3+1)-DIMENSIONAL CUBIC-QUINTIC CGL EQUATION

We analyze the nonlinear propagation of ultrashort electromagnetic pulses in uniform, bulk MMs, in which there are no free charges, and no fee currents flow, in the framework of the Maxwell's equations, written in differential form as

$$\nabla \times \mathbf{E} = -\frac{\partial \mathbf{B}}{\partial t}, \quad \nabla \times \mathbf{H} = \frac{\partial \mathbf{D}}{\partial t}, \quad \nabla \cdot \mathbf{D} = 0, \quad \text{and} \quad \nabla \cdot \mathbf{B} = 0, \tag{1}$$

where the quantities $\mathbf{E}$ and $\mathbf{H}$ are the electric and magnetic field vectors, respectively. The quantities $\mathbf{D}$ and $\mathbf{B}$ are the electric and magnetic flux densities, respectively. The induced polarization $\mathbf{P}$ and magnetization $\mathbf{M}$ may be made explicit in Maxwell's equations via the constitutive relations

$$\mathbf{D} = \varepsilon_0 \varepsilon \mathbf{E} + \mathbf{P}_{\mathrm{nl}}, \quad \text{and} \quad \mathbf{B} = \mu_0 \mu \mathbf{H} + \mathbf{M}_{\mathrm{nl}}, \tag{2}$$

were ε_0 and μ_0 are the permittivity and permeability of vaccum, respectively. ε and μ are dispersive complex permittivity and permeability of a dissipative medium. P_{nl} is a nonlinear polarization, and $\mathbf{M}_{\mathrm{nl}}$ is a nonlinear magnetization. $\mathbf{E}$, $\mathbf{D}$, $\mathbf{B}$, and $\mathbf{H}$ are slowly varying functions in space and time. The quasimonochromatic representation is used for the functions, namely $\mathbf{A}(r, t) = \mathbf{A} \exp(ikr - i\omega t)$, where ω is the carrier frequency and k is a complex vector. The first derivatives of Eqs. (2) with respect to time t are

$$\frac{\partial \mathbf{D}}{\partial t} = \varepsilon_0 (-i\omega \varepsilon \mathbf{E} - i\omega \varepsilon_{\mathrm{nl}} \mathbf{E}) e^{-i\omega t} \quad \text{and} \quad \frac{\partial \mathbf{B}}{\partial t} = \mu_0 (-i\omega \mu \mathbf{H} - i\omega \mu_{\mathrm{nl}} \mathbf{H}) e^{-i\omega t}. \tag{3}$$

We expand the dielectric permittivity $\varepsilon(\omega)$ and magnetic permeability $\mu(\omega)$ in Taylor series around the central frequency ω_0 as follows:

$$\omega \varepsilon(\omega) = \Sigma_{n=0}^{\infty} \left[\frac{\alpha_n}{n!} (\omega - \omega_0)^n \right], \quad \omega \mu(\omega) = \Sigma_{m=0}^{\infty} \left[\frac{\beta_m}{m!} (\omega - \omega_0)^m \right], \tag{4}$$

where $\alpha_n = \frac{\partial^n [\omega \varepsilon(\omega)]}{\partial \omega^n} \big|_{\omega=\omega_0}$ and $\beta_m = \frac{\partial^m [\omega \mu(\omega)]}{\partial \omega^m} \big|_{\omega=\omega_0}$. Substituting Eqs. (4) into Eqs. (3) yields

$$\frac{\partial \mathbf{D}}{\partial t} \approx \varepsilon_0 \left[-i\omega_0 \varepsilon \mathbf{E} + \alpha_1 \frac{\partial \mathbf{E}}{\partial t} + i\frac{\alpha_2}{2} \frac{\partial^2 \mathbf{E}}{\partial t^2} + \frac{\partial(\varepsilon_{\mathrm{nl}} \mathbf{E})}{\partial t} - i\omega_0 \varepsilon_{\mathrm{nl}} \mathbf{E} \right] e^{-i\omega t},$$

$$\frac{\partial \mathbf{B}}{\partial t} \approx \mu_0 \left[-i\omega_0 \mu \mathbf{H} + \beta_1 \frac{\partial \mathbf{H}}{\partial t} + i\frac{\beta_2}{2} \frac{\partial^2 \mathbf{H}}{\partial t^2} + \frac{\partial(\mu_{\mathrm{nl}} \mathbf{H})}{\partial t} - i\omega_0 \mu_{\mathrm{nl}} \mathbf{H} \right] e^{-i\omega t}. \tag{5}$$

Furthermore, we take the curl of Eqs. (1) and neglect vectorial terms such as $\nabla(\nabla.E) = 0$, using new variables $\xi = z$ and $\tau = t - \frac{1}{v_g}z$, where v_g is a real group velocity defined by $v_g = \left[\frac{\partial(n\omega)}{\partial\omega}\right]^{-1}$ and n is a negative-refractive index given by $n = -\sqrt{\text{Re}[\varepsilon\mu]} = k_r\frac{c}{\omega}$, with k_r being the negative wave vector's real part. This leads to

$$2ik\frac{\partial \mathbf{E}}{\partial \xi} + \Delta\mathbf{E} - \left(\frac{2}{v_g}\right)\frac{\partial^2 \mathbf{E}}{\partial \xi \partial \tau} - \frac{W}{c^2}\frac{\partial^2 \mathbf{E}}{\partial \tau^2} + i\frac{\omega_0^2}{c^2}\text{Im}[\varepsilon\mu]\mathbf{E} + \frac{\omega_0^2}{c^2}\mu\varepsilon_{\text{nl}}\mathbf{E} + i\frac{\omega_0}{c^2}(\mu + \beta_1)\frac{\partial(\varepsilon_{\text{nl}}\mathbf{E})}{\partial \tau}$$
$$- i\mu_0\frac{\partial(\mu_{\text{nl}}\mathbf{k}\times\mathbf{H})}{\partial \tau} - \mu_0\omega_0\mu_{\text{nl}}\mathbf{k}\times\mathbf{H} = 0, \tag{6a}$$

$$2ik\frac{\partial \mathbf{H}}{\partial \xi} + \Delta\mathbf{H} - \left(\frac{2}{v_g}\right)\frac{\partial^2 \mathbf{H}}{\partial \xi \partial \tau} - \frac{W}{c^2}\frac{\partial^2 \mathbf{H}}{\partial \tau^2} + i\frac{\omega_0^2}{c^2}\text{Im}[\varepsilon\mu]\mathbf{H} + \frac{\omega_0^2}{c^2}\mu_{\text{nl}}\varepsilon\mathbf{H} + i\frac{\omega_0}{c^2}(\varepsilon + \alpha_1)\frac{\partial(\mu_{\text{nl}}\mathbf{H})}{\partial \tau}$$
$$+ i\varepsilon_0\frac{\partial(\varepsilon_{\text{nl}}\mathbf{k}\times\mathbf{E})}{\partial \tau} + \varepsilon_0\omega_0\mathbf{k}\times\mathbf{E} = 0, \tag{6b}$$

where $W = -c^2 v_g^{-2} + \frac{1}{2}\omega_0(\mu\alpha_2 + \varepsilon\beta_2) + \alpha_1\beta_1$ is a complex function. To construct the ultrashort electromagnetic pulses in MMs for Eqs. (6), we assume both the electric and magnetic fields to propagate along the z direction, with the linearly polarized fields

$$\begin{pmatrix} \overrightarrow{E} \\ \overrightarrow{H} \end{pmatrix} = \begin{pmatrix} \widehat{x}E \\ \widehat{y}H \end{pmatrix} \exp[i(\beta_0 z - \omega_0 t)] + \text{c.c.}, \tag{7}$$

where ω_0 is the central frequency of the electromagnetic pulse, β_0 is the corresponding wave number, and c.c. denotes the complex conjugate. The nonlinear response of MMs is characterized by two different contributions. The first one is an intensity-dependent part of the effective dielectric permittivity of the MMs. The second contribution is the effective magnetic permeability which depends on the macroscopic magnetic field. For simplicity, the expression for the effective nonlinear dielectric permittivity is of the Kerr type. However, in order to prevent pulse collapse, the cubic nonlinearity (Kerr type) is usually saturated by a quintic nonlinearity with opposite sign, leading to

$$\varepsilon_{\text{nl}}(|E|^2) = \left[\varepsilon_r^{(3)} + i\varepsilon_i^{(3)}\right]|E|^2 - \left[\varepsilon_r^{(5)} + i\varepsilon_i^{(5)}\right]|E|^4, \tag{8}$$

and

$$\mu_{\text{nl}}(|H|^2) = \left[\mu_r^{(3)} + i\mu_i^{(3)}\right]|H|^2 - \left[\mu_r^{(5)} + i\mu_i^{(5)}\right]|H|^4. \tag{9}$$

We next substitute the expressions of $\varepsilon_{\text{nl}}(|E|^2)$ and $\mu_{\text{nl}}(|H|^2)$, given by Eqs. (8) and (9) into Eqs. (6), to get

$$i\frac{\partial E}{\partial z} + \frac{1}{2n\varpi}\Delta_\perp E + \frac{1}{2n\varpi}\frac{\partial^2 E}{\partial z^2} - \left(\frac{c}{n\varpi v_g}\right)\frac{\partial^2 E}{\partial z \partial t} - \frac{W}{2n\omega}\frac{\partial^2 E}{\partial \tau^2} + i\frac{\varpi}{2n}\text{Im}[\varepsilon\mu]E$$
$$+ \frac{\varpi}{2}\left\{\left[\chi_r^{(3)} + i\chi_i^{(3)}\right]|E|^2 E - \left(\chi_r^{(5)} + i\chi_i^{(5)}\right)|E|^4 E\right\} + \frac{I}{2}\left\{\left[\chi_r^{(3)} + i\chi_i^{(3)}\right]\frac{\partial(|E|^2 E)}{\partial t} - \left(\chi_r^{(5)} + i\chi_i^{(5)}\right)\frac{\partial(|E|^4 E)}{\partial t}\right\} = 0, \tag{10}$$

in which, for the purpose of simplification, the following normalized variables have been used [19] $\left(\frac{c}{\omega_p}\right)^2\Delta_\perp \to \Delta_\perp$, $\omega_p\tau \to t$, $\left(\frac{\omega_p}{c}\right)\xi \to z$, $\left(\frac{\omega_0}{\omega_p}\right) \to \varpi$, where ω_p is the plasma frequency. The cubic and quintic susceptibilities are given by $\chi^{(3)} = \varepsilon^{(3)}Z + \frac{\mu^{(3)}}{Z^{(3)}}$ and $\chi^{(5)} = \varepsilon^{(5)}Z + \frac{\mu^{(5)}}{Z^{(5)}}$, where $Z = \left(\frac{\mu}{\varepsilon}\right)^{\frac{1}{2}} = \frac{E}{H}$, is the medium impedance. We further calculate the first-order non-SVEA correction terms by using Eq. (10) to evaluate $\frac{\partial^2 E}{\partial z^2}$ and $\frac{\partial^2 E}{\partial z \partial t}$, and, neglecting higher-order terms, we have

$$\frac{\partial^2 E}{\partial z^2} \approx -C^2|E|^4 E, \quad \text{and} \quad \frac{\partial^2 E}{\partial z \partial t} \approx iC\frac{(|E|^2 E)}{\partial t} - iQ\frac{\partial(|E|^4 E)}{\partial t}, \tag{11}$$

where $C = \frac{\varpi}{2}\left[\chi_r^{(3)} + i\chi_i^{(3)}\right]$, $Q = \frac{\varpi}{2}\left[\chi_r^{(5)} + i\chi_i^{(5)}\right]$. Substituting Eqs. (11) into Eq. (10) leads to

$$i\frac{\partial E}{\partial z} + \sigma_\perp\Delta_\perp E + \sigma\frac{\partial^2 E}{\partial t^2} + \delta E + N_3|E|^2 E + N_5|E|^4 E + SS_3\frac{\partial(|E|^2 E)}{\partial t} + SS_5\frac{\partial(|E|^4 E)}{\partial t} = 0, \tag{12}$$

with the renormalization $\left(\sqrt{\frac{|2n\varpi|}{|\text{Re}[W]|}}\right)t \to t$, $\frac{\Delta_\perp}{2|n|\varpi} \to \Delta_\perp$, $\left(\frac{\sqrt{|\chi_r^{(3)}|\varpi}}{\sqrt{2}}\right)E \to E$, where the different coefficients are given in the Appendix. Equation (12) is the (3+1)D cubic-quintic CGL equation which models the propagation of ultrashort dissipative optical pulses in MMs, where $\sigma_\perp = (\sigma_{r\perp} + i\sigma_{i\perp})$ is the transverse complex coefficient, $\sigma = (\sigma_r + i\sigma_i)$ is the complex group-velocity dispersion (GVD). $\delta = (\delta_r + i\delta_i)$ is related to the linear loss($\delta < 0$) or gain ($\delta > 0$), while $N_3 = (N_{3r} + iN_{3i})$ and $N_5 = (N_{5r} + iN_{5i})$ are the cubic and quintic nonlinear complex coefficient, respectively. The complex parameters $SS_3 = (SS_{3r} + iSS_{3i})$ and $SS_5 = (SS_{5r} + iSS_{5i})$ characterize the so-called cubic and quintic SS effects due to cubic and quintic nonlinear polarizations,

respectively. The dielectric permittivity ε and magnetic permeability μ are dispersive in MMs and their frequency dispersion is described by the lossy Drude model of free-electron collisions (v_ε and v_μ) [76,77],

$$\varepsilon(\omega) = 1 - \frac{\omega_p^2}{\omega^2 + i\omega v_\varepsilon}, \quad \text{and} \quad \mu(\omega) = 1 - \frac{\omega_m^2}{\omega^2 + i\omega v_\mu}, \tag{13}$$

where ω_m is the magnetic plasma frequency [78].

III. MODULATIONAL INSTABILITY IN THE (3+1)-DIMENSIONAL CUBIC-QUINTIC CGL EQUATION FOR MMS

Some prototype of nonlinear evolution equations has been derived modeling driven nonlinear systems with dissipation and dispersion. Examples are the cubic CGL equation, which is an amplitude or envelope equation near a forward bifurcation to traveling waves, and the cubic-quintic CGL equation, which arises near the onset of a weakly inverted bifurcation associated with traveling waves [79–85]. Investigations of pattern formation problems can be understood quantitatively in terms of the Kuramoto-Sivashinsky equation, which is a nonlinear phase equation and describe the slowly varying phase of a plane wave well above the bifurcation, where amplitude equations are no longer applicable. The prototype of a nonlinear phase equation is the Kuramoto-Sivashinsky equation [86,87]. Sometimes, there is coupling between amplitude and phase equations. Furthermore, the Swift and Hohenberg equation [88] is an order parameter equation that contains a phenomenological aspect and whose use in the field of pattern formation is constructed such that it reduces to the appropriate envelope equation near the onset of the instability. With Benjamin-Feir-Newell phase diagram analysis, different states such as plane waves, phase turbulence, amplitude turbulence, bichaos, and spatiotemporal intermittency have been identified numerically [89–91]. Several parameters have been proposed that allows one to distinguish between the phase and amplitude turbulences, namely the density of defects, the phase and amplitude correlation lengths, and the Kaplan-Yorke dimension [92–94]. Nonetheless, the phase or amplitude turbulence is a scenario of some interest but is not a subject of study in this paper. Moreover, an essential extension of the theme has been done when those prototype of nonlinear evolution equations have been also well analyzed by many authors from different points of view (e.g., Painleve property, inverse scattering transform, Hirota direct method, and conservation laws), with special attention given to the study of soliton solutions [95–103]. As is well known, weak perturbations in the phase and/or the amplitude of a continuous wave (CW) or quasi-CW propagating in a nonlinear medium can grow exponentially into amplitude modulated waves at distinct modulation frequencies under certain conditions. This universal phenomenon, known as modulation instability (MI), is considered to be the precursor of soliton formation and is also closely related to the generation of rogue waves [104,105].

A. Linear stability analysis and gain spectrum

Physical, engineering, and biological sciences are continuously generating problems of either theoretical or practical interest. The necessary investigations of these problems in-

volve models that, very often, are mathematically expressed as ordinary differential equations (ODEs). In this respect, solving ODEs constitutes an important research activity which is ever attracting a great deal of attention. For instance, approximate solutions can be obtained analytically using various perturbation techniques for nonlinear ODEs which contain a small parameter. Problems with two or more scales of variation can be analyzed using the method of multiple scales [106] or the method of averaging [107]. In general, the starting point is the motivation in the choice of the ansatz. When a small parameter is zero, ODE has a sine or cosine periodic solution with the amplitude and phase constants. For small values of the small parameter, we expect the same form of the solution to be approximately valid, but now the amplitude and phase are expected to be slowly varying functions of time. The natural question is how the behavior of the amplitude and phase of the wave has been approached in PDEs.

Usually, the study of the linear stability starts by considering a plane-wave solution, especially in the case of MI. In this framework, we assume that Eq. (12) gets the exact CW solution

$$E(z, x, y, t) = Me^{i(k_1 x + l_1 y + k_z z - \omega_1 t)}, \tag{14}$$

where $|M|$ is positive real number representing the amplitude of the plane wave $E(z, x, y, t)$. k_1, l_1, and k_z are real numbers representing the wave vectors. ω_1 is real number representing the natural angular frequency of the plane wave. Making use of the above into Eq. (12) and setting both imaginary and real parts to zero, we obtain the dispersion relations

$$k_z - \sigma_{r\perp}(k_1^2 + l_1^2) - \omega_1^2 \sigma_r + \delta_r$$
$$+ M^2(N_{3r} + M^2 N_{5r}) + \omega_1 M^2(SS_{3i} + M^2 SS_{5i}) = 0,$$
$$- \sigma_{i\perp}(k_1^2 + l_1^2) - \omega_1^2 \sigma_i + \delta_i + M^2(N_{3i} + M^2 N_{5i})$$
$$- \omega_1 M^2(SS_{3r} + M^2 SS_{5r}) = 0. \tag{15}$$

The linear stability of the CW solution can be examined by introducing a small perturbation in the amplitude or in the phase or in both. Nevertheless, it has been shown in several occasions that even when amplitude and phase perturbations are simultaneously considered, the growth rate of instability mainly depends on the amplitude of the plane wave but it is independent of its wave vector and its frequency [108,109]. The latter relies on the fact that in the linearization process of the perturbed wave around the unperturbed one, there is always a possibility of finding a linear relationship between the phase and amplitude of the perturbation, which easily allows to control the emergence of instability around an amplitude threshold [108,109]. Zhao *et al.* [110], adopting the same procedure, confirmed that the emergence of nonlinear spin waves in an atomic chain of spinor Bose-Einstein condensates under MI mainly depends on the amplitude perturbation, even when both the phase and amplitude are perturbed. This finds real

applications in the field of gravitational waves, for example, where the carrier frequency is extremely high so that the sub-period power cannot be measured. In such conditions, the only measurable quantity remains the slowly varying amplitude of modulation [111]. Interestingly, phase and frequency modulation can indubitably become detectable only if converted into amplitude modulation [111]. Therefore, in the rest of this work, we consider an amplitude perturbation so that solution (14) becomes

$$E(z, x, y, t) = [M + a(z, x, y, t)]e^{i(k_1 x + l_1 y + k_z z - \omega_1 t)}, \quad (16)$$

where the complex field $a(x, y, z, t)$ is small perturbations of the carrier waves, i.e., $|a(x, y, z, t)| \ll |M|$. Next, we substitute Eq. (16) into Eq. (12) and keep only the terms that are linear in $a(x, y, z, t)$, which leads to the linearized equation of the perturbed field

$$
i\frac{\partial a}{\partial z} + \sigma_\perp \left[\Delta_\perp a + 2i\left(k_1 K \frac{\partial a}{\partial x} + l_1 L \frac{\partial a}{\partial y}\right)\right]
$$
$$
+ \sigma \frac{\partial^2 a}{\partial t^2} - 2i\omega_1 \sigma \frac{\partial a}{\partial t} + M^2(N_3 + 2M^2 N_5)(a + a^*)
$$
$$
+ M^2(2SS_3 + 3M^2 SS_5)\frac{\partial a}{\partial t} + M^2(SS_3 + 2M^2 SS_5)\frac{\partial a^*}{\partial t}
$$
$$
- i\omega_1 M^2(SS_3 + 2M^2 SS_5)(a + a^*) = 0. \quad (17)
$$

Here $a^*(x, y, z, t)$ is the complex conjugate of the perturbed field, assumed to be of the form

$$a(z, x, y, t) = a_1 e^{i(Kx + Ly + K_z z - \Omega t)} + a_2^* e^{-i(Kx + Ly + K_z z - \Omega^* t)}, \quad (18)$$

where K, L, and K_z are the perturbation wave numbers; Ω is the frequency of the perturbation modulating the carrier signal; and the parameters a_1 and a_2^* are constant complex amplitudes. The substitution of Eq. (18) into Eq. (17) gives a linear homogeneous system of equations in terms of a_1 and a_2,

$$
\begin{pmatrix} K_z + a_{11} & a_{12} \\ a_{21} & K_z + a_{22} \end{pmatrix} \begin{pmatrix} a_1 \\ a_2 \end{pmatrix} = \begin{pmatrix} 0 \\ 0 \end{pmatrix}, \quad (19)
$$

where

$$
a_{11} = \sigma_\perp(K^2 + L^2 + 2k_1 K + 2l_1 L) + \sigma(\Omega^2 + 2\Omega\omega_1)
$$
$$
- M^2(N_3 + 2M^2 N_5) + iM^2\Omega(2SS_3 + 3M^2 SS_5)
$$
$$
+ i\omega_1 M^2(SS_3 + 2M^2 SS_5),
$$

$$
a_{12} = -M^2(N_3 + 2M^2 N_5) + iM^2\Omega(SS_3 + 2M^2 SS_5)
$$
$$
+ i\omega_1 M^2(SS_3 + 2M^2 SS_5),
$$

$$
a_{21} = M^2(N_3^* + 2M^2 N_5^*) - iM^2\Omega(SS_3^* + 2M^2 SS_5^*)
$$
$$
+ i\omega_1 M^2(SS_3^* + 2M^2 SS_5^*),
$$

$$
a_{22} = -\sigma_\perp^*(K^2 + L^2 - 2k_1 K - 2l_1 L) - \sigma^*(\Omega^2 - 2\Omega\omega_1)
$$
$$
+ M^2(N_3^* + 2M^2 N_5^*) - iM^2\Omega(2SS_3^* + 3M^2 SS_5^*)
$$
$$
+ i\omega_1 M^2(SS_3^* + 2M^2 SS_5^*). \quad (20)
$$

The condition for the existence of nontrivial solution for the system (19) gives rise to a second-order polynomial equation for the wave number K_z that represents the dispersion law for

the perturbation, i.e.,

$$K_z^2 + sK_z + p = 0, \quad (21)$$

in which $s = a_{11} + a_{22}$ and $p = a_{11}a_{22} - a_{12}a_{21}$. We study the sign of the imaginary part of the roots of Eq. (21) and we investigate the gain or loss spectrum or the MI regions. This equation has two roots given by

$$K_z^{\pm} = \frac{1}{2}(-s \pm \sqrt{s^2 - 4p}). \quad (22)$$

The steady-state solution becomes unstable whenever the wave numbers $K_z^{\pm}$ have a nonzero imaginary part, since the perturbed amplitude grows exponentially along the NIM. The quantities $K_z^{\pm}$ depend on the values of the parameters that make the coefficients of the dispersion relation. Therefore, MI in NIMs, the presence of the wave numbers K and L of the perturbed mode, the wave number of the continuous wave k_1, cubic-quintic nonlinearities, and cubic and quintic self-steepening effects can be controlled. The regions of instability are called MI gain spectrums and are regions where the gain $G_+ = 2\text{Im}(K_z^+) > 0$, or $G_- = 2\text{Im}(K_z^-) > 0$, occur, where $\text{Im}(K_z^{\pm})$ represents the imaginary part of $K_z^{\pm}$.

Figure 1 displays some bounded regions of MI, with finite gains $G_- > 0$, and their corresponding density plots, versus the wave number K and k_1 of the perturbation and CW, respectively. The parameters used in the calculations are as follows: $\Omega = 0.6$, $\omega_1 = 0.8$, $L = -K$, $l_1 = 0.8$, $k_1 = 0.8$, $\sigma_\perp = -1 + i0.005$, $\sigma_i = 0.19$, $\delta = -0.081$, $SS_3 = -1 - i0.1$, and $SS_{5r} = 1$. In regions where $G_- > 0$, the plane wave will be expected to break up into nonlinear patterns and solitonic objects. Otherwise, the plane wave will remain stable under modulation. Such features of instability or stability are importantly modified by the changes in system parameters such as the cubic and quintic self-steepening coefficients. A good illustration of such effects is given by Fig. 2, where the MI gain G_- is plotted against the perturbation wave number K, with changing the cubic self-steepening coefficient SS_{3i}. In general, the MI gain spectrum is illustrated by two identical and symmetric lobes which get expanded when SS_{3i} decreases. This also affects the band gap which also grows when SS_{3i} decreases, while the MI gain decreases under the same effect. To remind, Fig. 2 has been plotted for $SS_{5i} = -0.44$, a value which does not give full information on how the MI gain can be affected by the quintic self-steepening term. This is illustrated in Fig. 3, where G_- is plotted versus K and SS_{5i}, both under anomalous and normal GVD regimes, with $SS_{3i} = -0.1$. As in Fig. 2, the Mi gain is characterized by two symmetric and identical lobes and, in general, G_- is a decreasing function of SS_{5i}. However, in the anomalous regime [see Fig. 3(a)], the band gap reduces with SS_{5i} increasing and solitons are not likely to exist when $SS_{5i} = 0$. On the other side, the normal GVD regime supports solitonic structures for $SS_{5i} = 0$ and the MI band gap is not considerable affected as in the anomalous GVD case. Indeed, this is contrary to what was already reported by Wen et al. [43]. In fact, they showed, using a (3+1)D NLS equation for ultrashort pulse propagation, that there was bandwidth amplification with increasing the cubic self-steepening parameter, in absence of the quintic nonlinear coefficient and the quintic self-steepening term. Moreover, the proposed model,
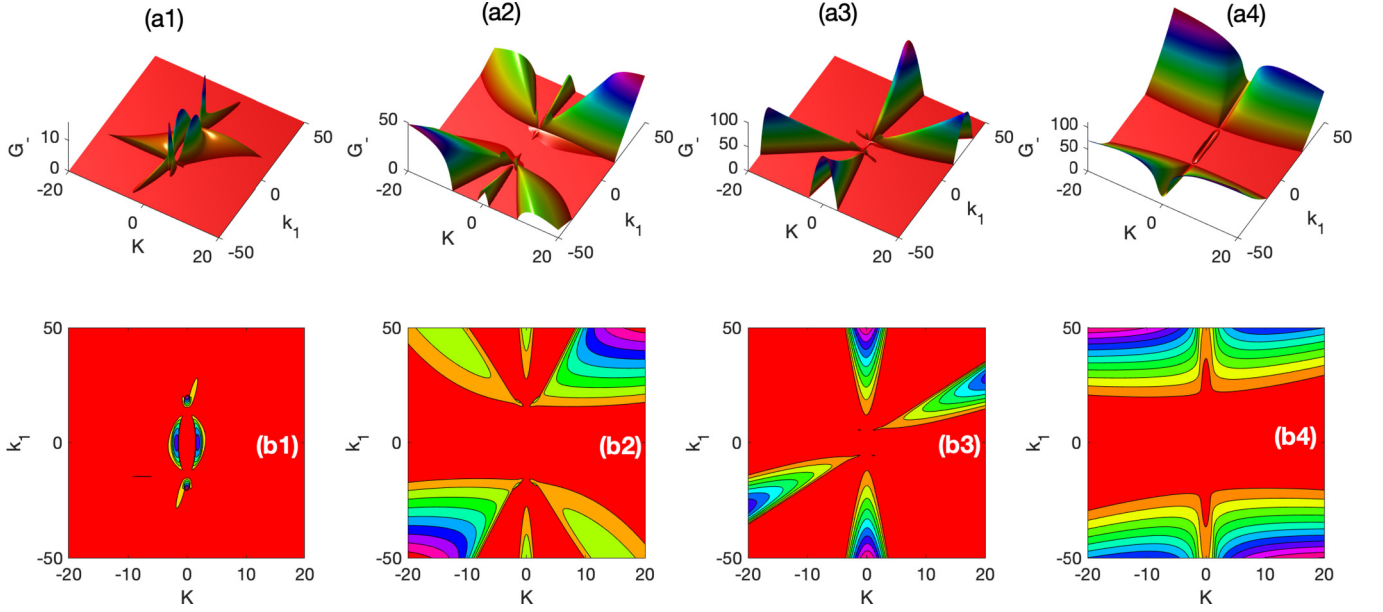
FIG. 1. Modulational instabilty gain associated with the solution G_- as a function of the wave number of the perturbation mode K and the wave number of the continuous wave k_1. Panels in (aj)$_{j=1,2,3,4}$ show bounded gains of MI, and the corresponding density plots in panels (bj)$_{j=1,2,3,4}$, for $\Omega = 0.6$, $\omega_1 = 0.8$, $L = -K$, $l_1 = 0.8$, $k_1 = 0.8$, $\sigma_{r\perp} = -1$, $\sigma_{i\perp} = 0.005$, $\sigma_i = 1.98$, $\delta_r = 0$, $\delta_i = -0.081$, $SS_{3r} = -0.4$, $SS_{3i} = 1.2$, $SS_{5r} = 0.5$, and $SS_{5i} = -0.9$. [(a1) and (b1)] normal GVD regime of self-focusing negative-index MMs, $\sigma_{r\perp} = -1$, $\sigma_r = 1$, $N_{3r} = 1$, $N_{3i} = -0.12$, $N_{5r} = -1$, and $N_{5i} = 0.075$; [(a2) and (b2)] anomalous GVD regime of self-defocusing negative-index MMs, $\sigma_{r\perp} = -1$, $\sigma_r = 1$, $N_{3r} = -1$, $N_{3i} = 0.12$, $N_{5r} = 1$, and $N_{5i} = -0.075$; [(a3) and (b3)] normal GVD regime of self-defocusing negative-index MMs, $\sigma_{r\perp} = -1$, $\sigma_r = 1$, $N_{3r} = -1$, $N_{3i} = 0.12$, $N_{5r} = 1$, and $N_{5i} = -0.075$; [(a4) and (b4)] anomalous GVD regime of self-defocusing positive-index MMs, $\sigma_{r\perp} = 1$, $\sigma_r = -1$, $N_{3r} = -1$, $N_{3i} = 0.12$, $N_{5r} = 1$, and $N_{5i} = -0.075$.

which contains essentially complex coefficient, is a generalized case, which, when $\sigma_i = \sigma_{i\perp} = \delta_I = \delta_r = N_{3i} = N_{5r} = N_{5i} = SS_{3r} = SS_{5i} = SS_{5r} = 0$, is recovered. Obviously, the balance between such new effects can modify the gain and be responsible for the emergence of more suitable patterns under long-time evolution.
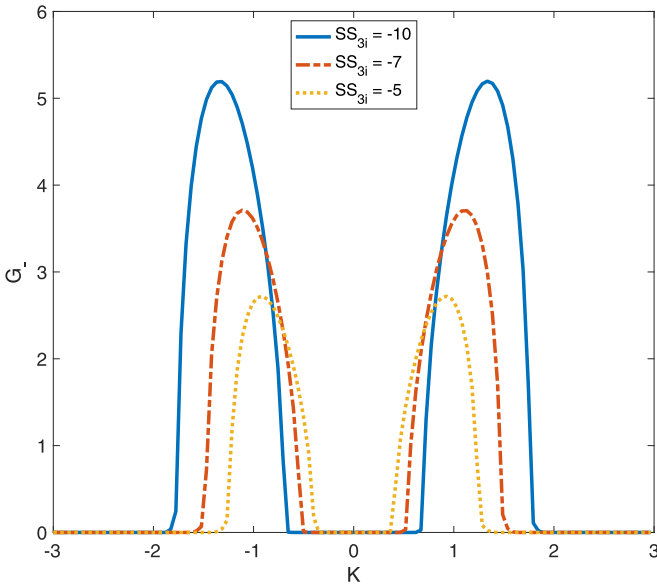
B. Numerical experiment

The linear stability analysis, which is based on the linearization around the unperturbed plane wave, is valid only when the amplitude of the perturbation is small compared to that of the carrier wave. More precisely, the linear approximation should not be valid at large timescales, since the amplitude of an unstable sideband grows exponentially. Therefore, the long-time evolution of the modulated plane wave requires full numerical simulations of the generic equation. This is, in fact, a way of confronting the analytical predictions and, in our context, pulse propagation in NIM is carried out via the split-step Fourier method on Eq. (12). In order to examine the accuracy of the performed digital experiment, different space and time steps are tested. Two hundred fifty-six space Fourier modes are used with the space period of 8, and in time the number of Fourier modes is also 256, with a similar period of 8. This corresponds to a simulation window of 8, both in space and time. Additionally, the numbers of grid points in space and time are 350 and 350, respectively, with the mesh size $\Delta x = \Delta y = 0.005$ and $\Delta t = 0.005$. The split-step Fourier method is then applied considering $y = 0$, with z constant, with the initial signal being of the form

FIG. 2. Plots of MI gain associated with solution G_-, versus K, for different values of SS_{3i} for $\Omega = 0.6$, $\omega_1 = 0.8$, $L = -K$, $l_1 = 0.8$, $k_1 = 0.8$, $\sigma_{r\perp} = -1$, $\sigma_{i\perp} = 0.005$, $\sigma_r = -1$, $\sigma_i = 0.19$, $\delta_i = -0.081$, $N_{3r} = -1$, $N_{3i} = 0.12$, $N_{5r} = 1$, $N_{5i} = -0.075$, $\delta_r = 0$, $SS_{3r} = -1$, $SS_{5r} = 1$, and $SS_{5i} = -0.44$.

$$E(x, t, 0) = M\{1 + A\sin[2\pi(\Omega_1 x + \Omega_2 t)]\}e^{-i(\omega_1 x + \omega_2 t)}, \quad (23)$$
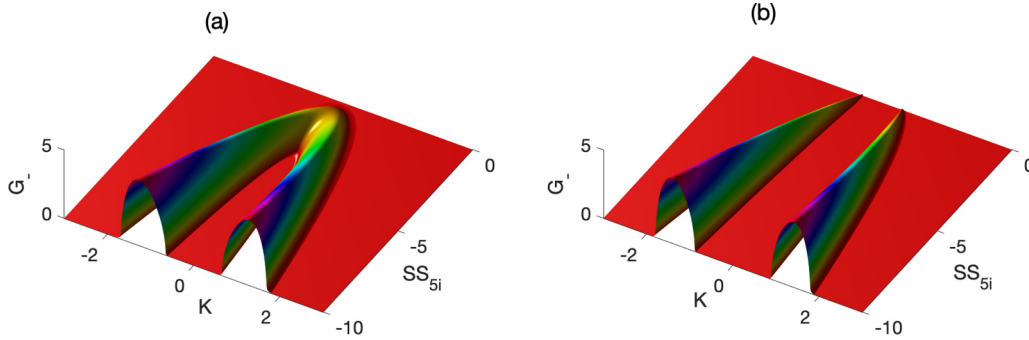
FIG. 3. Regions of MI illustrating gain associated with solution G_- against K, the wave number of perturbation, and the quintic self-steepening imaginary coefficient SS_{5i}, for $\Omega = 0.6$, $\omega_1 = 0.8$, $L = -K$, $l_1 = 0.8$, $k_1 = 0.8$, $\sigma_{r\perp} = -1$, $\sigma_{i\perp} = 0.005$, $\sigma_i = 0.19$, $\delta_r = 0$, $\delta_i = -0.081$, $N_{3i} = 0.12$, $N_{5r} = 1$, $N_{5i} = -0.075$, $SS_{3r} = -1$, $SS_{3i} = -0.1$, and $SS_{5r} = 1$. (a) Anomalous GVD regime of self-defocusing negative-index MMs, $\sigma_r = -1$ and $N_{3r} = -1$; (b) normal GVD regime of self-defocusing negative-index MMs, $\sigma_r = 1$ and $N_{3r} = -1$.

where A is modulation amplitude and Ω_1 and Ω_2 are the frequencies of weak sinusoidal modulations imposed on the continuous waves in the x and t directions, respectively.

According to features of Figs. 1–3, the development of MI depends on both the wave numbers K and self-steepening parameter values, which implies that right values of such parameters should be chosen to expect the appearance of soliton-like objects. While we use the parameter values $A = 0.001$, $\Omega_1 = \Omega_2 = 0.5$, $\omega_1 = \omega_2 = 0.41$, $\sigma_{r\perp} = -2.71$, $\sigma_{i\perp} = 0.5$, $\sigma_r = 2.57$, $\sigma_i = 0.5$, $\delta_r = 0$, $\delta_i = -0.0079$, $N_{3r} = -1$, $N_{3i} = .12$, $N_{5r} = 1$, $N_{5i} = -0.65$, $SS_{3r} = -0.2$, and $SS_{5r} = 0.42$, calculations are initiated for $SS_{3i} = -0.6$ and $SS_{5i} = -0.5$, which results in the MI behaviors summarized in Fig. 4, where, at distance $z = 5$, one clearly sees the appearance of a cluster of four fundamental solitons as the result of the interplay between nonlinear and dispersive effects. This, indeed, shows the accuracy of our analytical predictions and confirms that MI is a direct mechanism for soliton formation in nonlinear media. The most interesting aspect of the present numerical experiment is that the emerging entities are found to be moving as z increases, and their interaction leads to a complex molecular soliton [see Figs. 4(e) and 4(f)], which concentrates all the energies carries by individual solitons. Also, this brings out another main effect of MI, which is the creation of localized pulses and energy localization. In the past decades, different kinds of solitons have been discussed in the literature, along with their relationship with MI, including Bragg solitons, vortex solitons, discrete solitons, and cavity solitons [112], just to name a few. They are, however, few, the contributions that discuss the appearance of cluster solitons as the consequence of MI, a phenomenon that has, for instance, been related to azimuthal MI by Petroski *et al.* [113]. However, we should stress that intensive numerical studies have pointed out the fact that the stability of such structures is very sensitive to noise input [114], depending on the number of solitons composing the cluster, the angular quantum number of the azimuthal instability, and the corresponding largest growth rate of MI. Nevertheless, noise effects being not considered in the present paper, other aspects can be regarded as done in Fig. 5, where we have decreased the imaginary quintic self-steepening parameter to $SS_{5i} = -2$. As previously, the initial plane wave breaks into a four-wave

cluster of moving solitons which, as distance increases, merge into a unique structure [see Fig. 5(c)], gets more localized from distance $z = 15$ [see Fig. 5(d)]. Compared to the molecular structure of Fig. 4(f), which contains some humps, the unique molecular soliton of Fig. 5(d) displays some features of dromions that are well known in the literature [115,116]. As a whole, the numerical results discussed above show the strengths and weaknesses of our linear stability analysis of the MI in the (3+1)D CGL equation. It gives a correct conclusion about the analytical predictions, at least at the onset stage of wave evolution for a short distance of propagation. Indeed, for a sufficiently long distance and time, the linear stability analysis fails and the modulation can lead the system to the formation of localized patterns, spontaneously generated via wave-mixing processes during propagation and interaction. Indeed, such interactions, when they are inelastic, give rise to the complex molecular entities obtained from the model under study. From the physical point of view, the phenomenon displayed by Figs. 4(f) and 5(d) may result from the fact that the cubic and quintic self-steepening terms bring about additional nonlinear effects, which, because of the well-balanced effects between self-defocusing nonlinearity and dispersion, cause the rapid increase of pulse intensity, leading to maximum peaks. There are, however, two interesting behaviors of such maximum peak intensities, depending on the quintic self-steepening strength, that are pulse splitting in the temporal domain and compression in the spatial domain, on the one hand, and symmetric shrinking in both temporal and spatial domains, with the highest intensity being located at $(x = 0, t = 0)$ in both cases. In some other contexts, such behaviors may predict the emergence of spatial ring solitons that were reported in MMs by Zhang *et al.* [114] using a (3+1)D NLS equation, with simultaneous cubic electric and magnetic nonlinearity, by means of the variational method.

IV. CONCLUSION

A generalized (3+1)-dimensional cubic-quintic Ginzburg-Landau equation with self-steepening was investigated for the existence of MI regions. Following the standard procedure of linear stability analysis, the expression for the MI gain has been proposed and the effect of some keys parameters, such
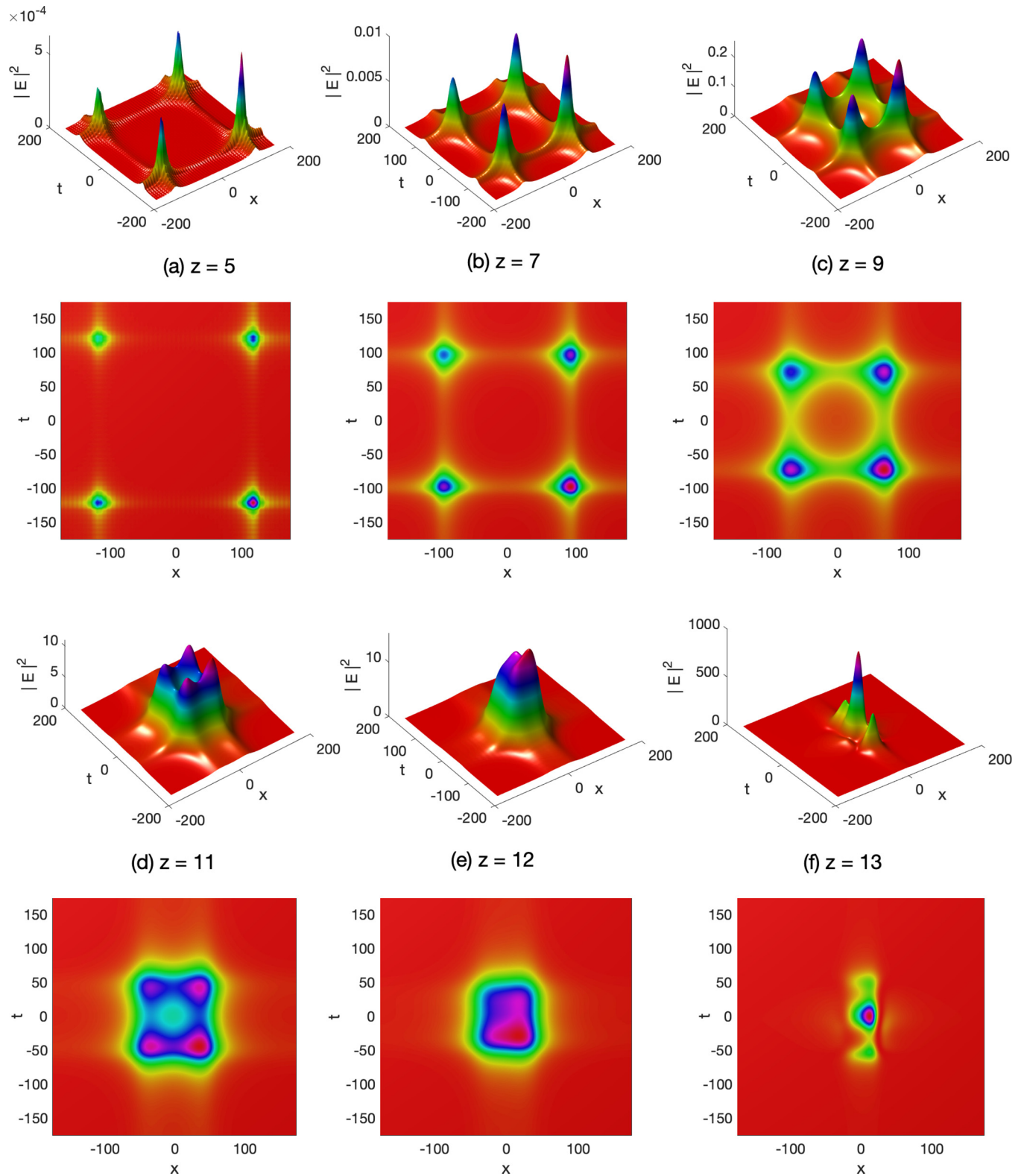
FIG. 4. Panels (a)–(f) show the structure of the beam intensity for a cluster of four fundamental solitons for different values of the longitudinal distance z and the corresponding density plots. (a) $z = 7$; (b) $z = 8$; (c) $z = 10$; (d) $z = 11$. The other parameter values are $A = 0.001$, $\Omega_1 = \Omega_2 = 0.5$, $\omega_1 = \omega_2 = 0.41$, $\sigma_{r\perp} = -2.71$, $\sigma_{i\perp} = 0.5$, $\sigma_r = 2.57$, $\sigma_i = 0.5$, $\delta_r = 0$, $\delta_r = -0.0079$, $N_{3r} = -1$, $N_{3i} = 0.12$, $N_{5r} = 1$, $N_{5i} = -0.65$, $SS_{3r} = -0.2$, $SS_{3i} = -0.6$, $SS_{5r} = 0.42$, and $SS_{5i} = -0.5$.
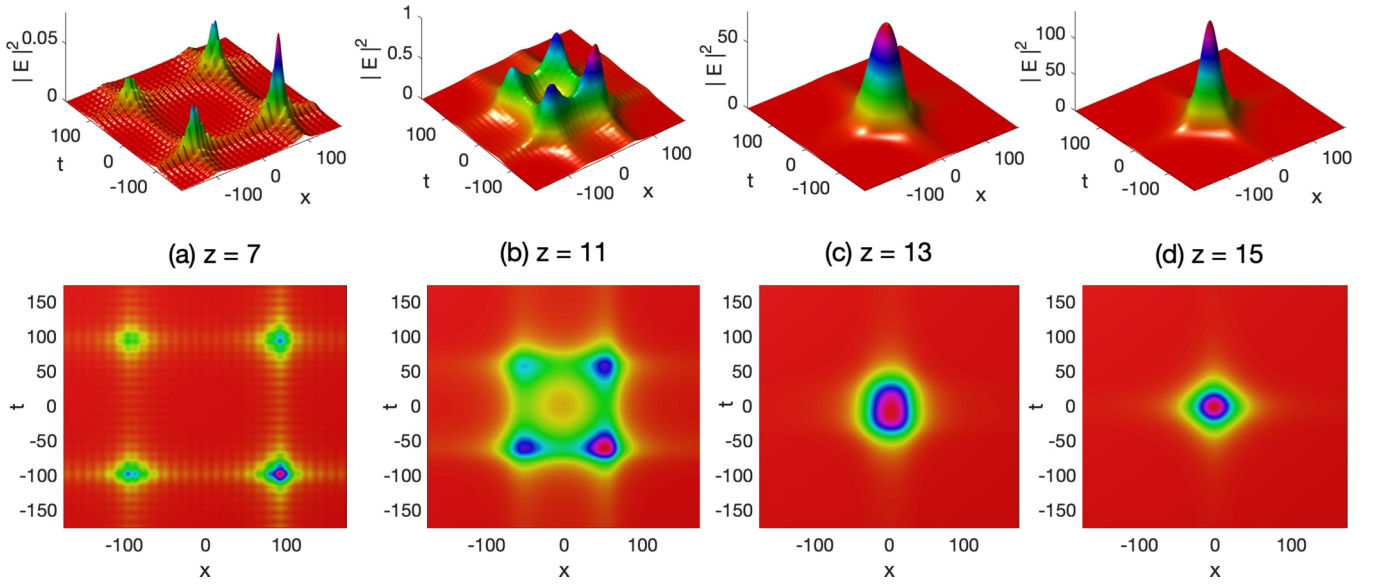
FIG. 5. Panels (a)–(d) show the structure of the beam intensity for a cluster of four fundamental solitons for different values of the longitudinal distance z and their corresponding density plots. (a) $z = 7$; (b) $z = 11$; (c) $z = 13$; (d) $z = 15$. The other parameter values used here are $A = 0.001$, $\Omega_1 = \Omega_2 = 0.5$, $\omega_1 = \omega_2 = 0.41$, $\sigma_{r\perp} = -2.71$, $\sigma_{i\perp} = 0.5$, $\sigma_r = 2.57$, $\sigma_i = 0.5$, $\delta_r = 0$, $\delta_r = -0.0079$, $N_{3r} = -1$, $N_{3i} = 0.12$, $N_{5r} = 1$, $N_{5i} = -0.65$, $SS_{3r} = -0.2$, $SS_{3i} = -0.6$, $SS_{5r} = 0.42$, and $SS_{5i} = -2$.

as the cubic and quintic self-steepening parameters, on the occurrence of MI has been addressed, both under anomalous and normal GVD regimes. The gain spectrum has revealed itself to be very sensitive to both self-steepening effects, which has been confirmed by direct numerical simulation, on the CQCGL equation, using the split-step Fourier method. Initially, the MI manifested itself by cluster of four fundamental pulses, which, with increasing distance, displayed some features of inelastic collision, leading to a single complex solitonic object. However, with decreasing the quintic self-steepening parameter, the resulting solitonic complex has been found to be more coherent, with a dromion-like shape.

Wen *et al.* [42] obtained a system of coupled equations which is suitable for any form of nonlinear polarization and magnetization. To make the propagation model applicable and solvable, some approximations have been made. (i) First, the SVEAs; (ii) the nonlinear polarization and nonlinear magnetization in the MM are of a Kerr-type; (iii) the frequency-dependent properties of the third-order electric and magnetic susceptibilities have been neglected for simplicity; (iv) the loss of medium has been neglected for simplicity; and, (v) finally, Wen *et al.* [42] obtained a system of coupled NLS equations, with mth-order linear and nonlinear dispersion terms, space-time focusing diffraction terms, cubic nonlinearity, cross-phase modulation, and the self-steepening effects resulting from the SVEA, respectively.

For comparison with the few-cycle pulse propagation model in a MM obtained by Wen *et al.* [42], we noticed the following points. We keep the linear dispersion coefficients to second order. We keep the first-order time derivative of the third- and fifth-order nonlinearities. We have considered the nonlinear polarization and nonlinear magnetization in the MM of a Kerr-type and of a non-Kerr quintic-type. In fact, based on the third-order Taylor expansion of the space-time focusing operator, Wen *et al.* [42], the second- and higher-order

nonlinear dispersions resulting from the linear dispersive permittivity and permeability can be neglected when we deal with the nonlinear propagation of few-cycle or wider pulses. At the meantime, the loss of medium has not been neglected. Thus, when a set of equations for the envelopes of the electric and magnetic fields is decoupled, the obtained propagation equation for the envelope of electric field is the cubic-quintic CGL equation. Generally speaking, this equation is essentially the cubic-quintic NLS equation with nonlinear gain and loss mechanisms, where both gain and loss are frequency and intensity dependent. This extension implies that the single balance between nonlinearity and dispersion is replaced by a composite balance between several effects. For instance, the balance between gain and loss, which should be exact in order to produce stationary localized solutions, plays a dominant role in the dynamics. For nonlinear propagation of ultrashort electromagnetic pulses with MMs, Wen *et al.* [42] have incorporated the linear dispersive permittivity and permeability into the nonlinear magnetization and polarization, resulting in the controllability of the SVEA *SS* parameter which is due to the variation of the ratio of phase velocity to group velocity with the central frequency of the pulse. The model equation that we have derived yields a corrected expression for the SVEA SS parameter, which essentially improves the description of the MI predicted by the improved growth rate spectrum for realistic MMs. In consequence, the obtained results, especially the emergence of clusters of localized pulses and their fusion over long propagation distance, make it possible to infer that a combination of competing cubic and quintic self-steepening terms can give rise to more complex behaviors, especially when there exists a suitable balance between such effects and dispersion, diffraction, loss, gain and cubic and quintic nonlinearities, some of the consequences being the formation of light bullets that constitute a hot topic in nonlinear optics nowadays.

ACKNOWLEDGMENTS

APPENDIX

The parameters of Eq. (12) are given by:

$$\sigma_{r\perp} = \text{sgn}(n), \quad \sigma_{i\perp} = 2\frac{-k_i}{k_r^2},$$

$$\sigma_r = \text{sgn}\left(-\frac{\text{Re}[W]}{n\varpi}\right), \quad \sigma_i = \frac{-\text{Im}[W]}{n\varpi\left|\left(-\frac{\text{Re}[W]}{n\varpi}\right)\right|},$$

$$\delta_r = 0, \quad w\delta_i = \frac{\varpi}{2n}\text{Im}[\varepsilon\mu],$$

$$N_{3r} = \text{sgn}\left(\chi_r^{(3)}\right), \quad N_{3i} = \frac{\chi_i^{(3)}}{\left|\chi_r^{(3)}\right|},$$

$$N_{5r} = \frac{-\chi_r^{(5)}}{\left|\chi_r^{(3)}\right|} - \frac{\chi_r^{(3)}\chi_r^{(3)} - \chi_i^{(3)}\chi_i^{(3)}}{4n\left|\chi_r^{(3)}\right|},$$

$$N_{5i} = \frac{-\chi_i^{(5)}}{\left|\chi_r^{(3)}\right|} - \frac{2\chi_r^{(3)}\chi_i^{(3)}}{4n\left|\chi_r^{(3)}\right|},$$

$$SS_{3r} = -\frac{1}{\varpi}\left(1 + \frac{1}{2nv_g}\right)\frac{N_{3i}}{\left|\left(-\frac{\text{Re}[W]}{n\varpi}\right)\right|},$$

$$SS_{3i} = \frac{1}{\varpi}\left(1 + \frac{1}{2nv_g}\right)\frac{N_{3r}}{\left|\left(-\frac{\text{Re}[W]}{n\varpi}\right)\right|},$$

$$SS_{5r} = -\frac{1}{\varpi}\left(1 + \frac{1}{2nv_g}\right)\frac{\chi_i^{(5)}}{\left|\left(-\frac{\text{Re}[W]}{n\varpi}\right)\right|\left|\chi_r^{(3)}\right|},$$

$$SS_{5i} = \frac{1}{\varpi}\left(1 + \frac{1}{2nv_g}\right)\frac{\chi_r^{(5)}}{\left|\left(-\frac{\text{Re}[W]}{n\varpi}\right)\right|\left|\chi_r^{(3)}\right|}$$

.

[1] J. B. Pendry, A. J. Holden, D. J. Robins, and W. J. Stewart, IEEE Trans. Microwave Theory Tech. **47**, 2075 (1999).

[2] S. O'Brien and J. B. Pendry, J. Phys.: Condens. Matter **14**, 4035 (2002).

[3] T. J. Yen, W. J. Padilla, N. Fang, D. C. Vier, D. R. Smith, J. B. Pendry, D. N. Basov, and X. Zhang, Science **303**, 1494 (2004).

[4] N. Katsarakis, G. Konstantinidis, A. Kostopoulos, R. S. Penciu, T. F. Gundogdu, M. Kafesaki, E. N. Economou, Th. Koschny, and C. M. Soukoulis, Opt. Lett. **30**, 1348 (2005).

[5] J. B. Pendry, A. J. Holden, W. J. Stewart, and I. Youngs, Phys. Rev. Lett. **76**, 4773 (1996).

[6] S. A. Ramakrishna, Rep. Prog. Phys. **68**, 449 (2005).

[7] J. B. Pendry, Contemp. Phys. **45**, 191 (2004).

[8] V. G. Veselago, Sov. Phys. Usp. **10**, 509 (1968).

[9] J. B. Pendry, Phys. Rev. Lett. **85**, 3966 (2000).

[10] R. A. Shelby, D. R. Smith, and S. Schultz, Science **292**, 77 (2001).

[11] D. Schurig, J. J. Mock, B. J. Justice, S. A. Cummer, J. B. Pendry, A. F. Starr, and D. R. Smith, Science **314**, 977 (2006).

[12] V. W. Shalaev, W. Cai, U. K. Chettiar, H.-K. Yuan, A. K. Sarychev, V. P. Drachev, and A. V. Kildishev, Opt. Lett. **30**, 3356 (2005).

[13] I. Kourakis, N. Lazarides, and G. P. Tsironis, Phys. Rev. E **75**, 067601 (2007).

[14] B. G. Onana Essama, J. Atangana, B. M. Frederick, B. Mokhtari, N. C. Eddeqaqi, and T. C. Kofane, Phys. Rev. E **90**, 032911 (2014).

[15] J. Atangana, B. G. Onana Essama, F. Biya Motto, B. Mokhtari, N. C. Eddeqaqi, and T. C. Kofané, J. Mod. Opt. **62**, 392 (2015).

[16] P. Y. Gouadjio Dontsop, B. G. Onana Essama, J. M. Dongo, M. Mbou Dedzo et al., Opt. Quantum Electron. **48**, 59 (2016).

[17] N. Lazarides and G. P. Tsironis, Phys. Rev. E **71**, 036614 (2005).

[18] I. S. Aranson and L. Kramer, Rev. Mod. Phys. **74**, 99 (2002).

[19] V. Skarka, N. B. Aleksic, and V. I. Berezhiani, Phys. Rev. A **81**, 045803 (2010).

[20] R. L. Fork, C. H. Brito Cruz, P. C. Becker, and C. V. Shank, Opt. Lett. **12**, 483 (1987).

[21] P. F. Curley, Ch. Spielmann, T. Brabec, F. Krausz, E. Wintner, and A. J. Schmidt, Opt. Lett. **18**, 54 (1993).

[22] J. Zhou, G. Taft, C.-P. Huang, M. M. Murname, H. C. Kapteyn, and I. Christov, Opt. Lett. **19**, 1149 (1994).

[23] T. Beddard, M. Ebrahimzadeh, D. T. Reid, and W. Sibbett, Opt. Lett. **25**, 1052 (2000).

[24] B. E. Schmidt, P. Béjot, M. Giguere, A. D. Shiner, C. Trallero-Herrero et al., Appl. Phys. Lett. **96**, 121109 (2010).

[25] A. Baltuska, Z. Wei, S. Pshenichnikov, and D. Wiersma, Opt. Lett. **22**, 102 (1997).

[26] J. E. Rothenberg, Opt. Lett. **17**, 1340 (1992).

[27] B. L. Holian, R. Blumenfeld, and P. Gumbsch, Phys. Rev. Lett. **78**, 78 (1997).

[28] C. Polymilis, D. J. Frantzeskakis, A. N. Yannacopoulos, K. Hizanidis, and G. Rowlands, J. Opt. Soc. Am. B **18**, 75 (2001).

[29] A. K. Sarma, Europhys. Lett. **92**, 24004 (2010).

[30] A. K. Sarma and P. Kumar, Appl. Phys. B **106**, 289 (2012).

[31] T. Brabec and F. Krausz, Phys. Rev. Lett. **78**, 3282 (1997).

[32] M. A. Porras, Phys. Rev. A **60**, 5069 (1999).

[33] P. Kinsler and G. H. C. New, Phys. Rev. A **67**, 023813 (2003).

[34] J. K. Ranka and A. Gaeta, Opt. Lett. **23**, 534 (1998).

[35] S. Tzortzakis, L. Sudrie, M. Franco, B. Prade, A. Mysyrowicz, A. Couairon, and L. Bergé, Phys. Rev. Lett. **87**, 213902 (2001).

[36] N. Akozbek, M. Scalora, C. M. Bowden, and S. L. Chin, Opt. Commun. **191**, 353 (2001).

[37] A. L. Gaeta, Opt. Lett. **27**, 924 (2002).

[38] M. Djoko and T. C. Kofané, Commun. Nonlin. Sci. Numer. Simulat. **48**, 179 (2017).

[39] M. Djoko and T. C. Kofané, Commun. Nonlin. Sci. Numer. Simulat. **68**, 169 (2019).

[40] M. Djoko and T. C. Kofané, Opt. Commun. **416**, 190 (2018).

[41] M. Djoko, C. B. Tabi, and T. C. Kofané, Phys. Scr. **94**, 075501 (2019)

[42] S. Wen, Y. Xiang, X. Dai, Z. Tang, W. Su, and D. Fan, Phys. Rev. A **75**, 033815 (2007).

[43] S. Wen, Y. Wang, W. Su, Y. Xiang, X. Fu, and D. Fan, Phys. Rev. E **73**, 036617 (2006).

[44] M. S. Syrchin, A. M. Zheltikov, and M. Scalora, Phys. Rev. A **69**, 053803 (2004).

[45] M. Scalora, M. S. Syrchin, N. Akozbek, E. Y. Poliakov, G. D'Aguanno, N. Mattiucci, M. J. Bloemer, and A. M. Zheltikov, Phys. Rev. Lett. **95**, 013902 (2005).

[46] Y. Xiang, X. Dai, S. Wen, J. Guo, and D. Fan, Phys. Rev. A **84**, 033815 (2011).

[47] A. K. Sarma, Eur. Phys. J. D **62**, 421 (2011).

[48] S. Sudo, H. Itoh, K. Okamoto, and K. Kubodera, Appl. Phys. Lett. **54**, 993 (1989).

[49] R. V. J. Raja, K. Porsezian, and K. Nithyanandan, Phys. Rev. A **82**, 013825 (2010).

[50] J. M. Chávez Boggio, S. Tenenbaum, and H. L. Fragnito, J. Opt. Soc. Am. B **18**, 1428 (2001).

[51] S. Liu, Appl. Phys. Lett. **89**, 171118 (2006).

[52] C. Martijn de Sterke, J. Opt. Soc. Am. B **15**, 2660 (1998).

[53] C. R. Phillips and M. M. Fejer, J. Opt. Soc. Am. B **27**, 2687 (2010).

[54] H. Ward, M. N. Ouarzazi, M. Taki, and P. Glorieux, Eur. Phys. J. D **3**, 275 (1998).

[55] A. Mohamadou, B. E. Ayissi, and T. C. Kofané, Phys. Rev. E **74**, 046604 (2006).

[56] F. II Ndzana, A. Mohamadou, and T. C. Kofané, Opt. Commun. **275**, 421 (2007).

[57] C. G. Latchio Tiofack, A. Mohamadou, T. C. Kofané, and A. B. Moubissi, Phys. Rev. E **80**, 066604 (2009).

[58] C. M. Ngabireng, S. Ambomo, P. T. Dinda, and A. B. Moubissi, J. Opt. **13**, 085201 (2011).

[59] L. M. Mandeng and C. Tchawoua, J. Opt. Soc. Am. B **30**, 1382 (2013).

[60] I. Kourakis and P. K. Shukla, Phys. Rev. E **72**, 016626 (2005).

[61] Y. Xiang, S. Wen, X. Dai, and D. Fan, Phys. Rev. E **82**, 056605 (2010).

[62] X. Dai, Y. Xiang, S. Wen, and D. Fan, J. Opt. Soc. Am. B **26**, 564 (2009).

[63] P. H. Tatsing, A. Mohamadou, C. Bouri, C. G. L. Tiofack, and T. C. Kofané, J. Opt. Soc. Am. B **29**, 3218 (2012).

[64] H. Zhuo, S. Wen, X. Dai, Y. Hu, and Z. Tang, Appl. Phys. B **87**, 635 (2007).

[65] M. Marklund, P. K. Shukla, and L. Stenflo, Phys. Rev. E **73**, 037601 (2006).

[66] S. Wen, Y. Xiang, W. Su, Y. Hu, X. Fu, and D. Fan, Opt. Express **14**, 1568 (2006).

[67] Y. Xiang, X. Dai, S. Wen, J. Guo, and D. Fan, J. Opt. Soc. Am. B **24**, 3058 (2007).

[68] W. Zhou, W. Su, X. Cheng, Y. Xiang, X. Dai, and S. Wen, Opt. Commun. **282**, 1440 (2009).

[69] A. Joseph, K. Porsezian, and P. Tchofo Dinda, J. Mod. Opt. **57**, 436 (2010).

[70] A. K. Sarma and M. Saha, J. Opt. Soc. Am. B **28**, 944 (2011).

[71] Y. Xiang, X. Dai, S. Wen, and D. Fan, J. Opt. Soc. Am. B **28**, 908 (2011).

[72] Y. Xiang, J. Wu, X. Dai, S. Wen, J. Guo, and Q. Wang, Opt. Express **20**, 26828 (2012).

[73] R. Gupta, T. S. Raju, C. N. Kumar, and P. K. Panigrahi, J. Opt. Soc. Am. B **29**, 3360 (2012).

[74] J. Zhang, Y. Xiang, S. Wen, and Y. Li, J. Opt. Soc. Am. B **31**, 45 (2014).

[75] X. Zhong, K. Cheng, and K. S. Chiang, J. Opt. Soc. Am. B **31**, 1484 (2014).

[76] A. A. Zharov, I. V. Shadrivov, and Y. S. Kivshar, Phys. Rev. Lett. **91**, 037401 (2003).

[77] A. Maluckov, Lj. Hadzievski, N. Lazarides, and G. P. Tsironis, Phys. Rev. E **77**, 046607 (2008).

[78] V. Skarka and N. B. Aleksic, Phys. Rev. Lett. **96**, 013903 (2006).

[79] A. C. Newell and J. A. Whitehead, J. Fluid Mech. **38**, 279 (1969).

[80] L. A. Segel, J. Fluid Mech. **38**, 203 (1969).

[81] H. R. Brand, P. S. Lomdahl, and A. C. Newell, Phys. Lett. A **118**, 67 (1986).

[82] H. R. Brand, P. S. Lomdahl, and A. C. Newell, Physica **23D**, 345 (1986).

[83] O. Thual and S. Fauve, J. Phys. (France) **49**, 1829 (1988).

[84] R. J. Deissler and H. R. Brand, Phys. Rev. Lett. **72**, 478 (1994).

[85] O. Descalzi and H. R. Brand, Phys. Rev. E **72**, 055202(R) (2005).

[86] Y. Kuramoto and T. Tsuzuki, Prog. Theor. Phys. **54**, 687 (1975).

[87] G. Sivashinsky, Acta Astronaut. **4**, 1177 (1977).

[88] J. Swift and P. C. Hohenberg, Phys. Rev. A **15**, 319 (1977).

[89] H. Chaté, Nonlinearity **7**, 185 (1994).

[90] J. B. Gonpe Tafo, L. Nana, and T. C. Kofané, Phys. Rev. E **88**, 032911 (2013).

[91] J. B. Gonpe Tafo, L. Nana, and T. C. Kofané, Phys. Rev. E **96**, 022205 (2017).

[92] D. A. Egolf and H. S. Greenside, Nature **369**, 129 (1994).

[93] T. Bohr, E. Bosch, and W. van de Water, Nature **372**, 48 (1994).

[94] D. A. Egolf and H. S. Greenside, Phys. Rev. Lett. **74**, 1751 (1995).

[95] N. R. Pereira and L. Stenflo, Phys. Fluids **20**, 1733 (1977).

[96] R. Conte and M. Musette, Physica D **69**, 1 (1993).

[97] P. Marcq, H. Chaté, and R. Conte, Physica D **73**, 305 (1994).

[98] E. Yomba and T. C. Kofané, J. Phys. Soc. Jpn. **69**, 1027 (2000).

[99] Y. Kuramoto and T. Tsuzuki, Prog. Theor. Phys. **55**, 356 (1976).

[100] G. I. Sivashinsky, Annu. Rev. Fluid Mech. **15**, 179 (1983).

[101] R. Conte and M. Musette, J. Phys. A **22**, 169 (1989).

[102] N. A. Kudryashov, Phys. Lett. A **147**, 287 (1990).

[103] K. Maruno, A. Ankiewicz, and N. Akhmediev, Physica D **176**, 44 (2003).

[104] G. P. Agrawal, *Applications of Nonlinear Fiber Optics* (Academic Press, New York, 2003).

[105] N. Akhmediev and A. Ankiewicz, Phys. Rev. E **83**, 046603 (2011).

[106] A. H. Nayfeh, *Introduction to Perturbation Techniques* (Wiley, New York, 1981).

[107] J. A. Sanders, F. Verhulst, and J. Murdock, *Averaging Methods in Nonlinear Dynamical Systems* (Springer, New York, 2007).

[108] T. Dauxois and M. Peyrard, *Physics of Solitons* (Cambridge University Press, Cambridge, UK, 2006).

[109] A. Kenfack Jiotsa and T. C. Kofané, J. Phys. Soc. Jpn. **72**, 1800 (2003).

[110] X.-D. Zhao, Z. W. Xie, and W. Zhang, Phys. Rev. B **76**, 214408 (2007).

[111] A. Freise, K. Strain, D. Brown, and C. Bond, Living Rev. Relat. **13**, 1 (2010).

[112] Y. S. Kivshar and G. P. Agrawal, *Optical Solitons: From Fibers to Photonic Crystals* (Academic Press, San Diego, CA, 2003).

[113] M. M. Petroski, M. S. Petrović, and M. R. Belić, Opt. Commun. **279**, 196 (2007).

[114] J. Zhang, S. Wen, Y. Xiang, Y. Wang, and H. Luo, Phys. Rev. A **81**, 023829 (2010).

[115] C. S. Panguetna, C. B. Tabi, and T. C. Kofané, Phys. Plasmas **24**, 092114 (2017).

[116] W. Liu, Y. Zhang, Z. Luan, Q. Zhou, M. Mirzazadeh, M. Ekici, and A. Biswas, Nonlin. Dyn. **96**, 729 (2019).